Naval Research Laboratory
Washington, DC 20375-5000

NRL Memorandum Report 6232

The Effect of First Reflections in the Dynamic Tear Test

VIRGINIA M. GENSHEIMER

Mechanics of Materials Branch
Materials Science and Technology Division

L. M. BROCK

Department of Engineering Mechanics
University of Kentucky
Lexington, KY 40506

M. I. JOLLES

Mechanics of Materials Branch
Materials Science and Technology Division

September 8, 1988

SECURITY CLASSIFICATION OF THIS PAGE

REPORT DOCUMENTATION PAGE

Form Approved
OMB No 0704-0188

1a. REPORT SECURITY CLASSIFICATION UNCLASSIFIED	1b. RESTRICTIVE MARKINGS
2a. SECURITY CLASSIFICATION AUTHORITY	3. DISTRIBUTION / AVAILABILITY OF REPORT Approved for public release; distribution unlimited.
2b. DECLASSIFICATION / DOWNGRADING SCHEDULE	
4. PERFORMING ORGANIZATION REPORT NUMBER(S) NRL Memorandum Report 6232	5. MONITORING ORGANIZATION REPORT NUMBER(S)
6a. NAME OF PERFORMING ORGANIZATION Naval Research Laboratory 6b. OFFICE SYMBOL (If applicable) Code 6382	7a. NAME OF MONITORING ORGANIZATION
6c. ADDRESS (City, State, and ZIP Code) Washington, DC 20375-5000	7b. ADDRESS (City, State, and ZIP Code)
8a. NAME OF FUNDING / SPONSORING ORGANIZATION Office of Naval Research 8b. OFFICE SYMBOL (If applicable) ONR	9. PROCUREMENT INSTRUMENT IDENTIFICATION NUMBER
8c. ADDRESS (City, State, and ZIP Code) Arlington, VA 22217	10. SOURCE OF FUNDING NUMBERS PROGRAM ELEMENT NO: 61153N22 / PROJECT NO: RR022-01-48 / TASK NO: / WORK UNIT ACCESSION NO: DN480-509

11. TITLE (Include Security Classification)
The Effect of First Reflections in the Dynamic Tear Test

12. PERSONAL AUTHOR(S)
Gensheimer, V.M., Brock,* L.M. and Jolles, M.I.

13a. TYPE OF REPORT	13b. TIME COVERED	14. DATE OF REPORT (Year, Month, Day)	15. PAGE COUNT
	FROM _____ TO _____	1988 September 8	26

16. SUPPLEMENTARY NOTATION
*Department of Engineering Mechanics, University of Kentucky, Lexington, KY 40506

17. COSATI CODES			18. SUBJECT TERMS (Continue on reverse if necessary and identify by block number)
FIELD	GROUP	SUB-GROUP	Dynamic fracture, Dynamic tear test, Finite element, Elastic response, Stress waves

19. ABSTRACT (Continue on reverse if necessary and identify by block number)

The dynamic tear (DT) test if often used to study dynamic fracture. Previous work has indicated that the first impact waves arriving at the specimen notch may not create a stress state severe enough for fracture. In this article, a finite element program for the exact dynamic simulation of an actual DT test is first compared with an analytical solution for the time interval prior to reflected wave appearance. The finite element results are then used to study the exact stress field near the specimen notch. This study demonstrates that is is the arrival of the first reflected waves at the notch which generate the stress field necessary for fracture. These results are then used to estimate a critical dynamic stress intensity factor value for the DT test.

20. DISTRIBUTION / AVAILABILITY OF ABSTRACT ☒ UNCLASSIFIED/UNLIMITED ☐ SAME AS RPT ☐ DTIC USERS	21. ABSTRACT SECURITY CLASSIFICATION UNCLASSIFIED
22a. NAME OF RESPONSIBLE INDIVIDUAL Virginia M. Gensheimer	22b. TELEPHONE (Include Area Code) (202) 767-9027 22c. OFFICE SYMBOL Code 6382

DD Form 1473, JUN 86 Previous editions are obsolete. SECURITY CLASSIFICATION OF THIS PAGE

S/N 0102-LF-014-6603

CONTENTS

THE EFFECT OF FIRST REFLECTIONS IN THE DYNAMIC TEAR TEST

Introduction

Dynamic brittle fracture studies are often (Timoshenko, 1913; Mason, 1936; Lee, 1940; Eringen, 1953; Nash and Lange, 1969; Zehnder and Rosakis, 1986) based on the dynamic tear (DT), or three-point bend, test. In this test, a mass impacts the unnotched side of a simply-supported, notched rectangular bar, and the resulting elastic wave diffraction at the notch causes fracture there. As indicated schematically in Fig. 1, test dimensions can be chosen so that the mass strikes more or less uniformly across the bar width, and complete symmetry exists with respect to the notch plane. Because the notch gap is small, the wave-induced stress state at the notch is, then, approximately that of a Mode I crack.

The elastic waves are not treated explicitly in studies such as those referenced above, perhaps in part because of the mathematical difficulty inherent in problems whose solution requires the coupling of dilatational and rotational waves in geometries which feature corners and characteristic lengths, see for example Miklowitz (1982). However, as pointed out by Kolsky (1973), and demonstrated analytically by Brock and Rossmanith (1985) and Brock (1986), the arrival of specific waves can have a pronounced effect on a crack tip stress field. As a first step in accounting for the elastic waves arising in the DT test, a transient, two-dimensional analysis was performed by Brock, Jolles and Schroedl (1985), hereafter known as BJS. The analysis used an impact time history determined experimentally by Nash and Lange (1969), hereafter known as NL, and yielded exact solutions for times prior to the arrival of reflected waves. The bar cross-section at the notch was found to go into compression when the first dilatational wave from the mass impact arrived. The normal stress on the cross section then peaked in compression, and subsequently became tensile. This tensile state occurred just prior to the arrival of the first impact-generated rotational wave, and grew rapidly thereafter. However,

Manuscript approved May 4, 1988.

the occurence coincided roughly with what would have been the arrivals of the first reflected waves had they been included in the analysis. Moreover, even without them, the Mode I dynamic stress intensity factor did not reach any value thought (Shockey, Kalthoff, Klemm and Winkler, 1983) to be critical for brittle fracture until well after the experimentally-determined (NL) fracture initiation time.

These results indicated that reflected waves probably generate the stress state necessary to cause brittle fracture at the notch, and that the arrival of the earlier reflected waves is an important event in the critical stress state generation.

In order to move beyond the conjectural nature of these results, and to shed light on the critical value of the dynamic stress intensity factor, this article extends the work of BJS by performing an analysis of the NL DT test which can account for the effect of both impact and reflected waves. As in BJS, the test is modeled as a rectangular, simply supported bar subjected to a uniform line load across the bar width. It is assumed that a plane strain state exist, that the bar remains fixed to the supports and that the notch is essentially a Mode I crack tip. Once again, the actual impact history obtained in NL is used to determine the line load.

A finite element (FE) program is used to solve the full transient problem and results are compared with those obtained by an analysis similar to that used in BJS in the time interval prior to the arrival of reflected waves; in that interval the anlaysis is, of course, exact. While the FE program does not treat individual waves, the mesh and code adopted satisfy rather strict error bounds, and guarantee accurate, numerically stable results.

From the FE solution, stress field histories are obtained, and are compared with the reflection-free histories to confirm the observations of BJS concerning wave reflection effects. An FE-based dynamic stress intensity

factor is then used to estimate the value critical for fracture.

In the next section, the reflection-free case is described, and expressions for the normal stress components presented. In BJS, only the dynamic stress intensity factor was actually given. In the sequel, the particular FE process used for the complete problem is described, and some results presented. The FE/reflection-free comparison and the estimation of the critical dynamic stress intensity factor follow.

Reflection-free solutions

Consider the cracked half-plane shown in Fig. 2: The assumptions that plane strain exists in the bar of Fig. 1 and that the mass impact can be represented by a time-varying line load P imply that, until the elastic impact waves are reflected from the ends and notched side of the bar, the total bar disturbance can be represented in the geometry of Fig. 2. In Fig. 2, we see that the impact waves are those which radiate from the impact site, and those which result from the subsequent diffraction at the crack tip. There, h represents the ligament length at the notch plane in the bar. The parameter s is the time t after impact initiation multiplied by the dilatational wave speed, while m is that speed non-dimensionalized with respect to the rotational wave speed. The half-plane is, like the bar, assumed to be linearly elastic, isotropic and homogeneous.

If we now further restrict our time of interest to exclude the reflection of the impact waves from the impact, i.e. half-plane, surface itself, then the solution at any point will be the superposition of the two elastic impact wave ensembles shown in Fig. 2.

In essence, this solution was obtained by BJS by adapting a scheme introduced by Freund (1974) for dynamic crack problems which exhibit a characteristic length in the crack plane. However, as noted earlier, only the dynamic

stress intensity factor was actually given, and to calibrate the FE study, complete expressions for the stresses are required. These are presented, therefore, below:

The impact wave ensemble shown in Fig. 2a constitutes the solution to a two-dimensional Lamb's problem (Lamb, 1904) for a time-varying line load (point force in the plane). This problem has been considered both in BJS and by Achenbach (1973). Extension of those results and rewriting them in terms of the more convenient coordinate systems indicated in Fig. 2a yields for $x \geq 0, y < h$ the normal stress components

$$\pi\sigma_x = \int_d^s \mathrm{Re}\left[\frac{\tau a}{pR}(m^2-2a^2)\right]_1 + \int_\rho^s \mathrm{Re}\left(\frac{4q^2b^2a}{pR}\right)_2 \cdot \dot{P}(s-\tau)d\tau \tag{1}$$

$$\pi\sigma_y = \int_d^s \mathrm{Re}\left(\frac{\tau^2 a}{pR}\right)_1 - \int_\rho^s \mathrm{Re}\left(\frac{4q^2b^2a}{pR}\right)_2 \cdot \dot{P}(s-\tau)d\tau \tag{2}$$

Here Re( ) and Im( ) denote the real and imaginary parts of a complex function, $(\dot{})$ denotes s-differentiation, and a subscript j implies that the terms in parentheses are functions of (p_j, q_j), where

$$d^2q_1 = i\tau x + (h-y)p_1, \quad p_1 = \sqrt{(\tau^2-d^2)} \tag{3}$$

$$d = \sqrt{[x^2 + (h-y)^2]} \tag{4}$$

while

$$d^2q_2 = -i\tau x + (h-y)p_2, \quad p_2 = \sqrt{|\tau^2-m^2d^2|}, \quad \rho = md \tag{5}$$

for $d > mx$. For $mx > d$, however,

$$\rho = x + (h-y)\sqrt{(m^2-1)} > mr \tag{6}$$

which requires that

$$id^2q_2 = \tau x + (y-h)p_2 \tag{7}$$

when $md>\tau$. In eqns (1) and (2),

$$a = \sqrt{(1+q^2)}, \quad b = \sqrt{(m^2+q^2)} \tag{8}$$

$$T = b^2+q^2, \quad R = 4q^2ab-T^2 \tag{9}$$

where R is the Rayleigh function, and it is understood that $Re(a,b)\geq 0$ in the q-plane with branch cuts $Re(q)=0$ and $|Im(q)|>1$, $|Im(q)|>m$, respectively.

The impact wave ensemble in Fig. 2b shown radiating from the crack tip is due to the diffraction of the ensemble considered above. In BJS, it was found that tne former could be obtained as a weighted superposition of the latter. Extension of these results yields, therefore, expressions for the normal stress σ_x when $x>0$ in the form

$$\pi^2\sigma_x = -\int_{r+h}^{s} \int_{1}^{\frac{1}{h}(\tau-r)} F_1 - \int_{h+\rho}^{s} \int_{1}^{\frac{1}{h}(\tau-\rho)} F_2 \cdot QS_1 dk\dot{P}(s-\tau)d\tau$$

$$-\int_{mh+r}^{s} \int_{m}^{\frac{1}{h}(\tau-r)} F_1 - \int_{mh+\rho}^{s} \int_{m}^{\frac{1}{h}(\tau-\rho)} F_2 \cdot QS_2 dk\dot{P}(s-\tau)d\tau \tag{10}$$

where $F_j=F_j(p_j,q_j)$ and

$$r^2q_1 = iy(\tau-kh)+xp_1, \quad p_1 = \sqrt{[(\tau-kh)^2-r^2]} \tag{11}$$

$$r = \sqrt{(x^2+y^2)} \tag{12}$$

while

$$r^2q_2 = iy(\tau-kn)+xp_2, \quad p_2 = \sqrt{|(\tau-kh)^2-m^2r^2|}, \quad \rho = mr \tag{13}$$

for $r>-my$. For $my>-r$, however,

$$\sigma = -y+x\sqrt{(m^2-1)} > mr \tag{14}$$

which requires that

$$ir^2 a_2 = -y(\tau-kh)-xp_2 \tag{15}$$

when $mr>\tau$. The functions $F_j(p,q)$ themselves are defined as

$$2(1-m^2)pF_1 = -Re(T^2M_+) \tag{16}$$

$$2(1-m^2)pF_2 = Re(4q^2b^2M_+) \tag{17}$$

where

$$M_+ = \frac{\sqrt{(1-iq)}}{(n-iq)(k-iq)G_+} \tag{18}$$

$$\ln G_+ = -\frac{1}{\pi}\int_1^m \frac{du}{u+iq}\tan^{-1}\left(\frac{4u^2\alpha B}{K^2}\right) \tag{19}$$

$$\alpha = \sqrt{(u^2-1)}, \quad B = \sqrt{(m^2-u^2)}, \quad K = m^2-2u^2 \tag{20}$$

and (T,a,b) are given again by eqns (8) and (9), with (a,b) defined in the same cut q-plane. We can obtain the expression for σ_y from eqn. (10) by replacing F_2 with its negative, and by replacing eqn. (16) with the definition

$$2(1-m^2)pF_1 = -Re[(m^2-2a^2)TM_+] \tag{21}$$

For both σ_x and σ_y, the functions $Q(k)$, $S_j(k)$ are given by

$$Q(k) = \frac{\sqrt{(1+k)}}{(k+n)G(k)} \tag{22}$$

$$\ln G(k) = -\frac{1}{\pi}\int_1^m \frac{du}{u+k}\tan^{-1}\left(\frac{4u^2\alpha B}{K^2}\right) \tag{23}$$

$$\sqrt{(k^2-1)}S_1 = \frac{kMK}{4k^2\alpha\sqrt{(k^2-1+m^2)}-M^2}, \quad M = 2k^2-2+m^2 \tag{24}$$

$$S_2 = \frac{4\beta k^2\sqrt{(k^2-m^2+1)}}{4\beta^2 k\sqrt{(k^2-m^2+1)}-K^2}, \quad \beta = \sqrt{(k^2-m^2)} \tag{25}$$

Finally, 1/n is the Rayleigh wave speed non-dimensionalized with respect to the dilatational wave speed; it is obtained from the zeroes $q = \pm in$ of R.

Experimental impact load

Impact tests leading to the brittle fracture of A517 steel bars in the Fig. 1 configuration have been performed (NL), and the time history of the impact force measured. A plot of this history is given in Fig. 3. In BJS, this time history was found to be accurately represented by a line load P, uniform across the bar width, with the time response

$$P(s) = \frac{F_o}{c_1} s[1+ \frac{3}{10}(\frac{s}{s_p}) - \frac{8}{15}(\frac{s}{s_p})^2] \tag{26}$$

$$s_p = 0.35m, \quad c_1 = 5790 \text{ m/sec}, \quad F_o = 1.4(10^5)\text{MN/m-sec} \tag{27}$$

where s=0 is the start of impact, s_p corresponds to the instant of peak impact force, and c_1 is the dilatational wave speed in the bar. In addition, the dimensionless wave speed parameters for the bar were found to have the values

$$m = 1.84, \quad n = 1.987 \tag{28}$$

For the NL DT test specimen, h=28.6 mm, so that $s_p \sim 12h$, and the time of fracture is $s \sim 14h$.

Substitution of eqn. (26) into the expressions given in the previous section yields, therefore, the normal stresses at points within the bar which are free of reflected waves. These expressions are exact solutions of the governing equations, yet involve the actual NL impact time history. It should be noted that, in terms of h, eqn. (26) is valid for $0<s<14h$, the first impact waves arising from notch diffraction reach the impact region at $s = 2h$ and,

for the bars used in BL, the first reflected waves to reach the notch are from the notched side of the NL bar and arrive at s~1.39h. Therefore, eqn. (26) itself includes the effects of wave reflections and, strictly speaking, the expressions for σ_x and σ_y are valid for $0<s<1.89h$.

Finite Element Program Outline

The FE code ABAQUS (Hibbit, Karlsson and Sorensen, 1984) is used to computationally simulate the DT test. Symmetry with respect to the notch plane requires that only half of the specimen by modeled. This half is represented by a mesh consisting of 1539 nodes and 1456 CPE4H elements. The latter are identical plane strain square elements, 1.588 mm on a side, with linear displacement interpolation, and an independent hydrostatic stress component (Hibbit, Karlsson and Sorensen, 1984b). This component is coupled to the constitutive relationship for the specimen material by LaGrange multipliers. The use of such a hybrid element is required in regions of large deformation in order to eliminate artificial stiffening caused by the propagation of unrealistic nodal displacement constraints through the mesh. In order to avoid localized element crushing, besides, the line load defined by eqs. (26) and (27) is actually represented as a uniform pressure spanning two elements.

It should be noted, further, that the mesh does not include special elements which could model a crack tip, i.e. notch, singularity.

In regard to its execution, ABAQUS uses an explicit integration scheme, whereby quantities at time t_i are determined as functions of the same quantities at time t_{i-1}. To eliminate numerical instabilities associated with time-step changes within the integration scheme, the Hilber-Hughes-Taylor single-parameter operator is employed, with a damping factor of -0.05.

In order to avoid unwieldly trial-and-error convergence checks to determine the permissable time-step size, ABAQUS provides an analytical method: The solution is calculated at time t_{i+1} based on an initial time-step size. The residual of the momentum balance equations are then determined at time $t_i + \Delta t/2$. The relative value of this half-step residual is generally inversely proportional to solution accuracy, so that the original Δt can be adjusted to control solution stability. The error bounds for the half-step residuals are based on the expected nodal forces. The original time-step is reduced and the solution at t_{i+1} recalculated if the half-step residuals are not within the prescribed limits.

The maximum possible time-step size Δt is based on elemental characteristic dimensions and material wave speed. In the present analysis, the initial time-step is chosen to be the maximum possible time step.

$$\Delta t = d^*/c_2 \tag{29}$$

where c_2 is the rotational wave speed and d^* is the minimum dimension of the smallest mesh element. This time-step is consistent with that employed in another time-dependent three-point bend analysis (Nakamura, Shih and Freund, 1986). No reduction in time-step was found to be necessary for solution stability in the present analysis.

Geometric nonlinearities due to large strains and rotations are included in the present analysis. However, material nonlinearity is not required, as the properties for A517 steel listed here indicate:

Young's modulus E: 206.8 GPa
Shear modulus μ: 75.8 GPa
Poisson's ratio ν: 0.27
dilutational wave speed c_1: 5790 m/sec
rotational wave speed c_2: 3147 m/sec

Finite Element Calculations

As the list of properties, Fig. 3 and eq. (27) show, the NL-based line load reaches its peak at t=60.46 μsec($s=s_p$) where, of course, t=0(s=0) is the instant of initial impact. For purposes of incorporating the effects of

at least the first dilatational and rotational waves and notch surface Rayleigh waves (Brock and Rossmanith, 1985) generated by reflections from the notched surface of the specimen, it is sufficient to model the DT test from t=0 to t=28.5 μsec. As examples of the FE results generated, the four non-zero stresses along the line y=0,x>0 from the crack tip near the arrival times of the first impact wave (5.32 μsec) and the first reflection (9.88 μsec) are shown in Figs. 4 and 5, respectively. The variations with t of the Mode I opening stress σ_x a small distance (1.32 mm) from the crack tip along the radial lines $\theta=0$ and $\theta=\pi/2$ are shown in Fig. 6.

To study the Mode I dynamic stress intensity factor K_I, the classical (Sneddon and Lowengrub, 1969) result for a stationary semi-infinite crack is used:

$$K_I = \lim_{r\to 0} \sqrt{(2\pi r)}\, \frac{\sigma_x}{f(\theta)}\,, \quad f(\theta) = \cos\frac{1}{2}\left(\frac{\pi}{2}-\theta\right)\left[1+\sin\frac{1}{2}\left(\frac{\pi}{2}-\theta\right)\sin\frac{3}{2}\left(\frac{\pi}{2}-\theta\right)\right] \qquad (30a,b)$$

Because, the FE mesh does not contain a singularity-producing element, K_I cannot be obtained directly from the FE data. However, good agreement between FE and analytical results has been shown when the limiting process of eq. (30a) is performed by graphical extrapolation (Broek, 1982). From such extrapolations at various times during the interval $0<t<28.5$ μsec, it is possible to develop the K_I time history shown in Fig. 7.

Comparison of Analytical and FE Solution

A partial calibration of the FE program can be obtained by comparing its numerical results with those generated by the analytical solution given above. A typical and rather severe comparison is shown in Fig. 8, where the crack-opening stress σ_x on the notch plane (= /2) very near (r=1.32 mm) the crack tip is plotted vs. time. There is no disturbance at this point until the first

impact wave arrives at t=4.9 μsec. The first reflected wave arrives at t=9.4 μsec, at which time the analytical results are, of course, no longer exact. In view of this, Fig. 8 shows excellent agreement until this time and, indeed, somewhat beyond it. In particular, both solutions show clearly the intial compression of the notch region. Fig. 8 also shows that after t~11 μsec, the analytical results begin to seriously underestimate the magnitude of the notch stress state. This clearly indicates the importance of the reflected wave arrivals in determining this state and, in turn, confirms the conjectures of BJS.

Estimate of Critical Stress Intensity Factor

As mentioned at the outset, the BJS-based dynamic stress intensity factor K_I did not achieve a range of values deemed critical for fracture until well after the experimentally-determined (NL) fracture initiation time. The observations made above about Fig. 8 show, of course, why this was so, and we now turn to the FE results to estimate a critical value of K_I. Extrapolation of the K_I-curve in Fig. 7 out to the NL-estimated fracture initiation time t=70 μsec gives K_I~144 $MN/m^{3/2}$. This value is higher than the critical range adopted in BJS. However, that range was based on zero-velocity extrapolations of intensity factor data found for growing cracks, e.g. (Shockley, Kalthoff, Klemm and Winkler, 1983). Similar experiments which examine K_I near fracture initiation have, however, been performed for 4340 steel (Zehnder and Rosakis, 1986). There, K_I is found to be in the range 200-250 $MN/m^{3/2}$ at 5 μsec after fracture, but to drop rapidly afterwards.

Brief Discussion

This paper presented another step in the full transient study of a dynamic tear (DT), or three-point bend, brittle fracture test modeled as a process of

plane strain. As in a previous step (Brock, Jolles and Schroedl, 1985), a major goal of this paper was to accurately determine the role of elastic wave arrivals at the test specimen notch in generating the stress state necessary for dynamic fracture to occur.

An FE code, ABAQUS, with capabilities for treating exact dynamic equations was first compared with the analytical solution which is exact for times prior to the arrival of wave reflections. The FE results were then used to examine the test model behavior during the interval in which the specimen notch receives first reflections from the notched side of the specimen. This behavior established clearly that it is such reflections, and not the initial impact waves, which generate the stress state critical for dynamic fracture.

The time history of the dynamic stress intensity factor could also be obtained graphically from the FE results, and extrapolation of this history to the experimentally-determined (Nash and Lange, 1969) fracture initiation time yielded an estimate for the critical value. This value was in qualitative agreement with values obtained from other, similar, tests.

With the importance of the first reflected waves thus established, future work will anlayze the test model results near the actual time of fracture initiation. More importantly, perhaps, future work will incorporate the possibility of material nonlinearity, so that the test model interpretation no longer need be restricted to purely brittle fracture.

Acknowledgement
This work was performed while one of the authors (LMB) was a Senior Summer Faculty Fellow at the Naval Research Laboratory, under the Navy/ASEE Summer Faculty Research Program. The work was supported entirely by the Naval Research Laboratory.

References

Achenbach, J. D., 1973, Wave Propagation in Elastic Solids, North-Holland, Amsterdam, pp. 303-309.

Broek, D., 1982, Elementary Engineering Fracture Mechanics, Martinus Nijhoff, Boston, pp. 330-338.

Brock, L. M., 1986, "The Transient Field under a Point Force Acting on an Infinite Strip," ASME Journal of Applied Mechanics, Vol. 53, pp. 321-325.

Brock, L. M., Jolles, M., and Schroedl, M., 1985, "Dynamic Impact over a Subsurface Crack: Applications to the Dynamic Tear Test," ASME Journal of Applied Mechanics, Vol. 52, pp. 287-290.

Brock, L. M., and Rossmanith, H. P., 1985, "Analysis of the Reflection of Point Force-Induced Crack Surface Waves by a Crack Edge," ASME Journal of Applied Mechanics, Vol. 52, pp. 57-61.

Eringen, A. C., 1953, "Transverse Impact on Beams and Plates," ASME Journal of Applied Mechanics, Vol. 20, pp. 461-468.

Freund, L. B., 1974, "The Stress Intensity Factor due to Normal Impact Loading on the Faces of a Crack," International Journal of Engineering Science, Vol. 12, pp. 179-190.

Hibbit, H. D., Karlsson, B. I. and Sorensen, E. 1984a ABAQUS User's Manual, Hibbit, Karlsson and Sorensen, Inc., Providence, RI.

Hibbit, H. D., Karlsson, B. I. and Sorensen, E. 1984b ABAQUS Theory Manual, Hibbit, Karlsson and Sorensen, Inc., Providence, RI.

Kolsky, H., 1973, "Recent Work on Relations between Stress Pulses and Fracture," in Dynamic Crack Propagation, Sih, G. C., ed., Noordhoff, Leyden, pp. 399-414.

Lamb, H., 1904, "On the Propagation of Tremors over the Surface of an Elastic Solid," Philosophical Transactions of the Royal Society, London, Series A, Vol. 203, pp. 1-42.

Lee, E. H., 1940, "Impact of a Mass Striking a Beam," Transactions of the ASME, Vol. 62, pp. A129-A138.

Mason, H. L., 1936, "Impact on Beams," Transactions of the ASME, Vol. 58, pp. A55-A61.

Miklowitz, J., 1982, "Wavefront Analysis in the Nonseperable Elastodynamic Quarter-Plane Problems, I Part 1: The General Method," ASME Journal of Applied Mechanics, Vol. 49, pp. 797-807.

Nakamura, T., Shih, C. F., and Freund, L. B., 1986, "Analysis of a Dynamically Loaded Three-Point Bend Ductile Fracture Specimen," Engineering Fracture Mechanics, Vol. 25, pp. 323-339.

Nash, G. E., and Lange, E. A., 1969, "Mechanical Aspects of the Dynamic Tear Test," ASME Journal of Basic Engineering, Vol. 91, pp. 535-543.

Shockey, S. A., Kolthoff, J. F., Klemm, W., and Winkler, S., 1983, "Simultaneous Measurements of Stress Intensity and Toughness for Fast-Running Cracks," Experimental Mechanics, Vol. 23, pp. 140-145.

Sneddon, I. N., and Lowengrub, M., 1969, Crack Problems in the Classical Theory of Elasticity, John Wiley & Sons, New York.

Timoshenko, S. P., 1913, "Zur Frage nach der Wirkung eines Stoff auf einen Balken," Zeitschrift für Mathematik und Physik, Vol. 62, pp. 198-209.

Zehnder, A. T., and Rosakis, A. J., 1986, "Dynamic Fracture Initiation and Propagation in 4340 Steel under Impact Loading," SM Report 86-6, Graduate Aeronautical Laboratories, California Institute of Technology.

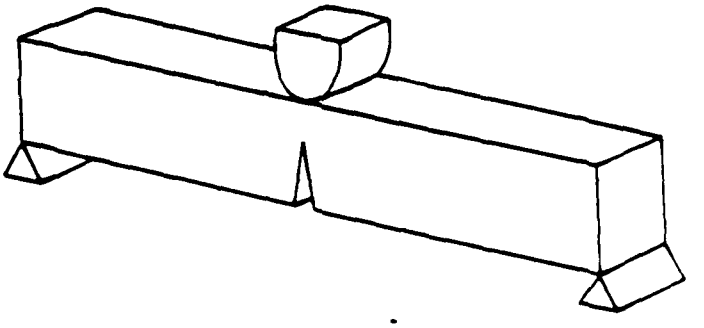

Figure 1 DT-test schematic

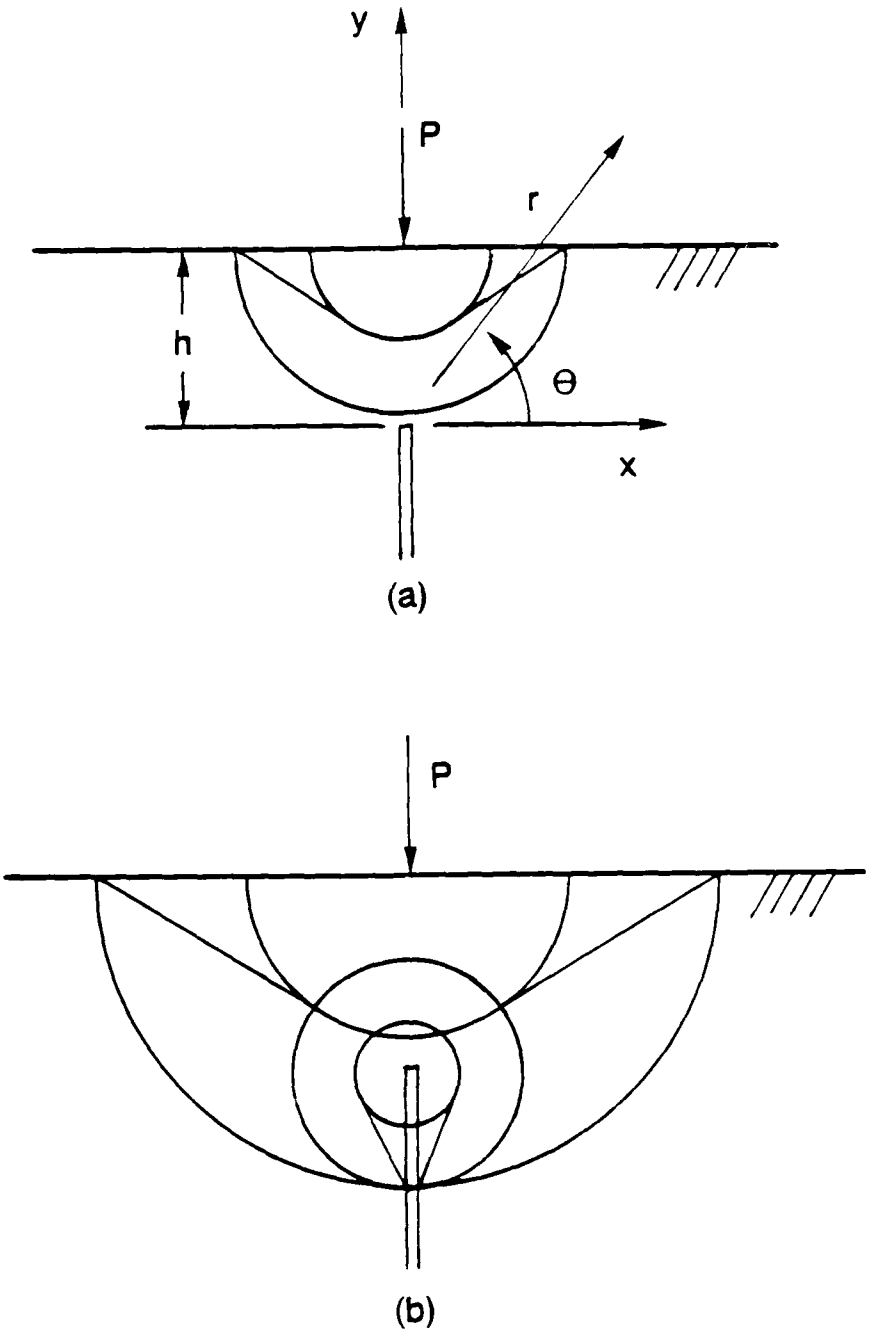

Figure 2 Reflection-free solution geometry

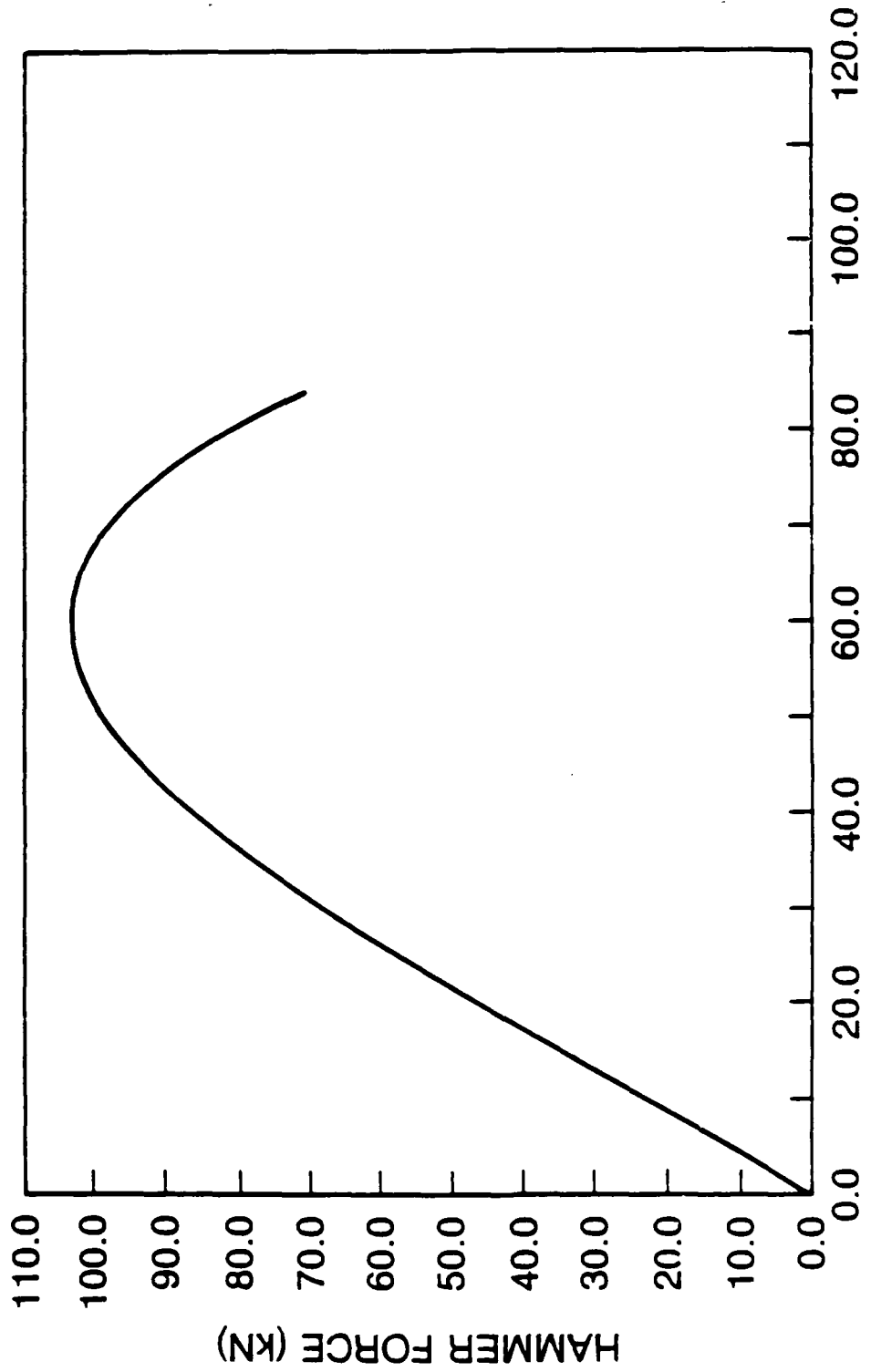

Figure 3 Impact load history

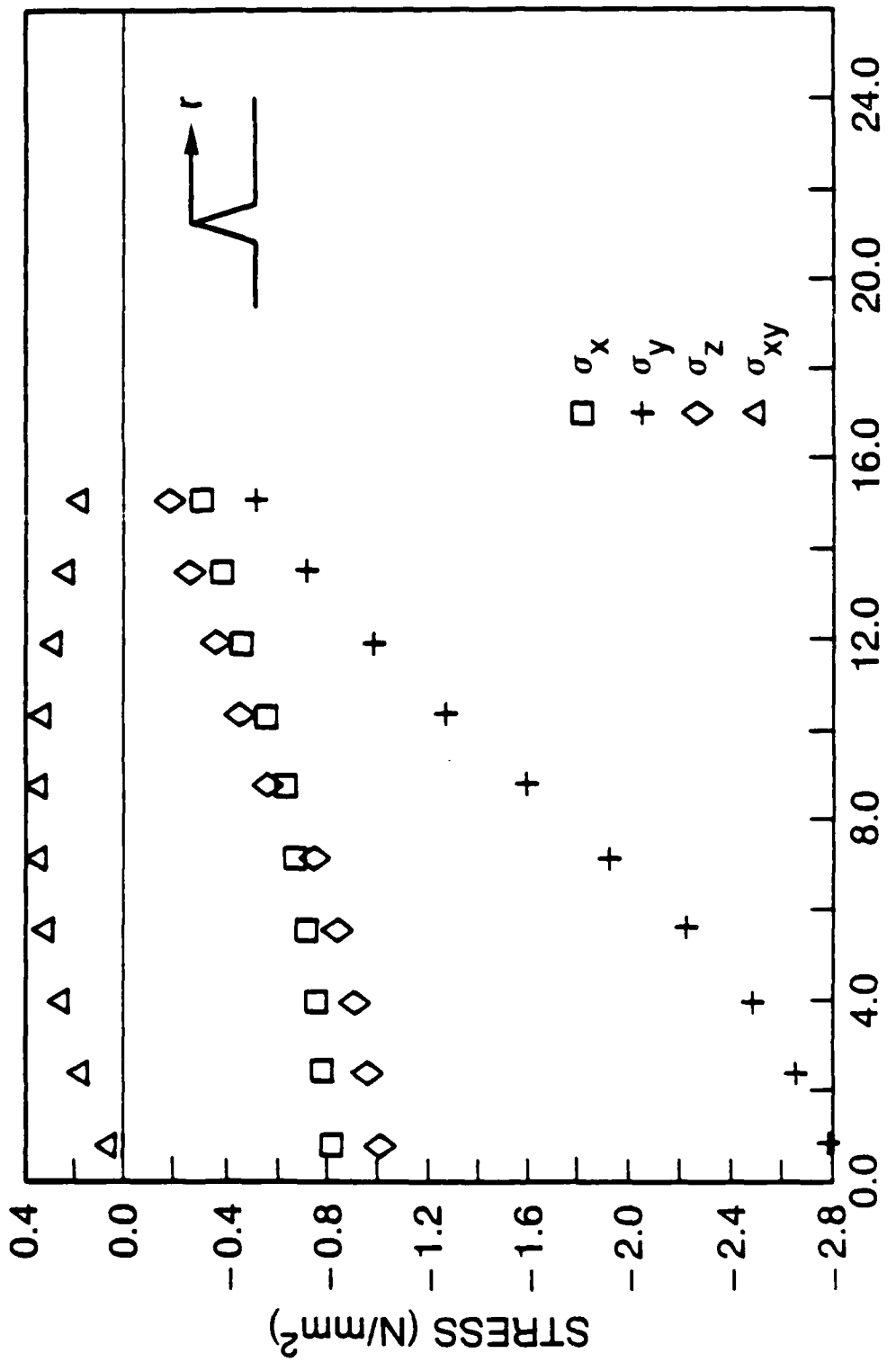

Figure 4 Stress near notch(crack tip) at 5.32×10^{-6} sec

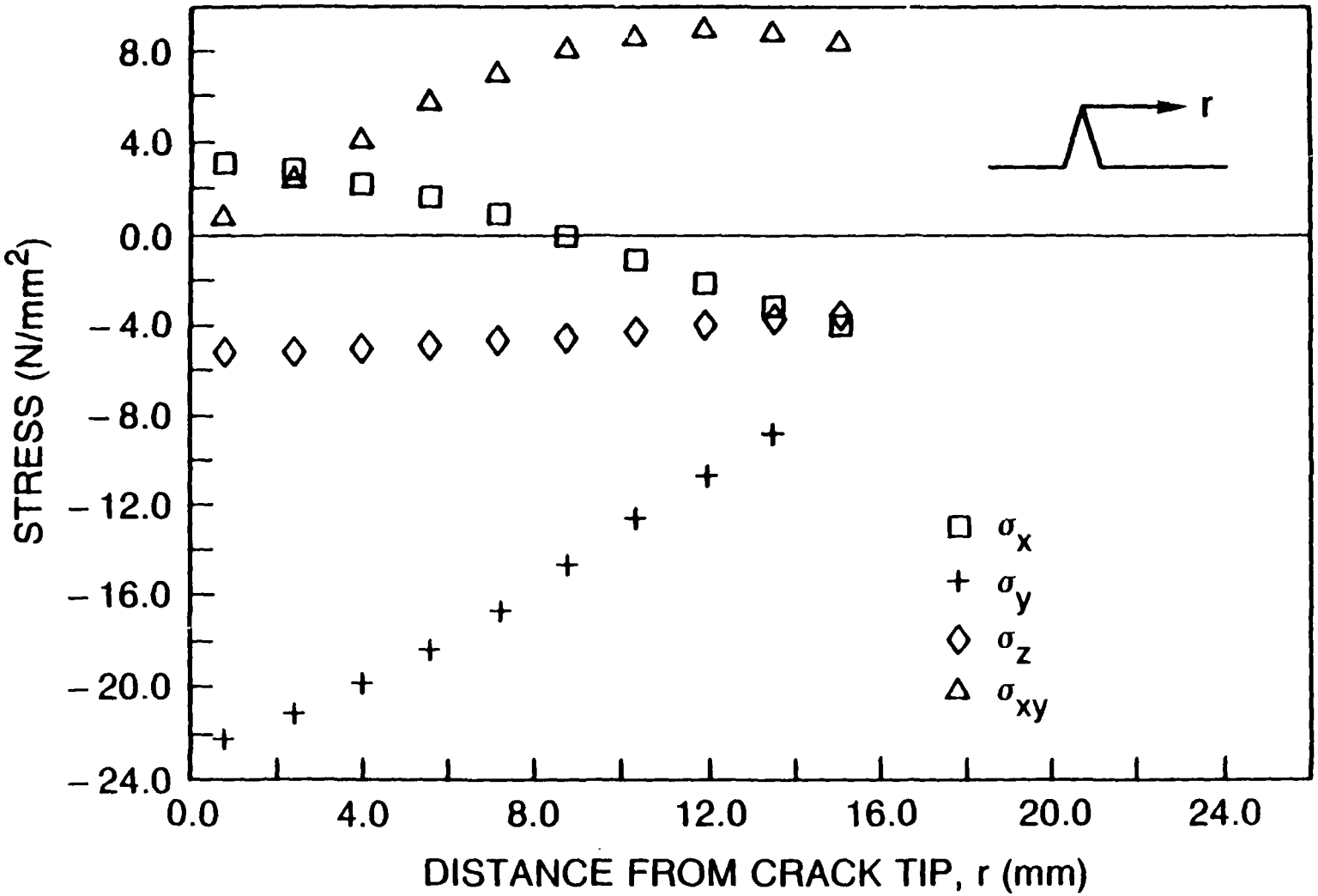

Figure 5 Stress near notch(crack tip) at 9.88×10^{-6} sec

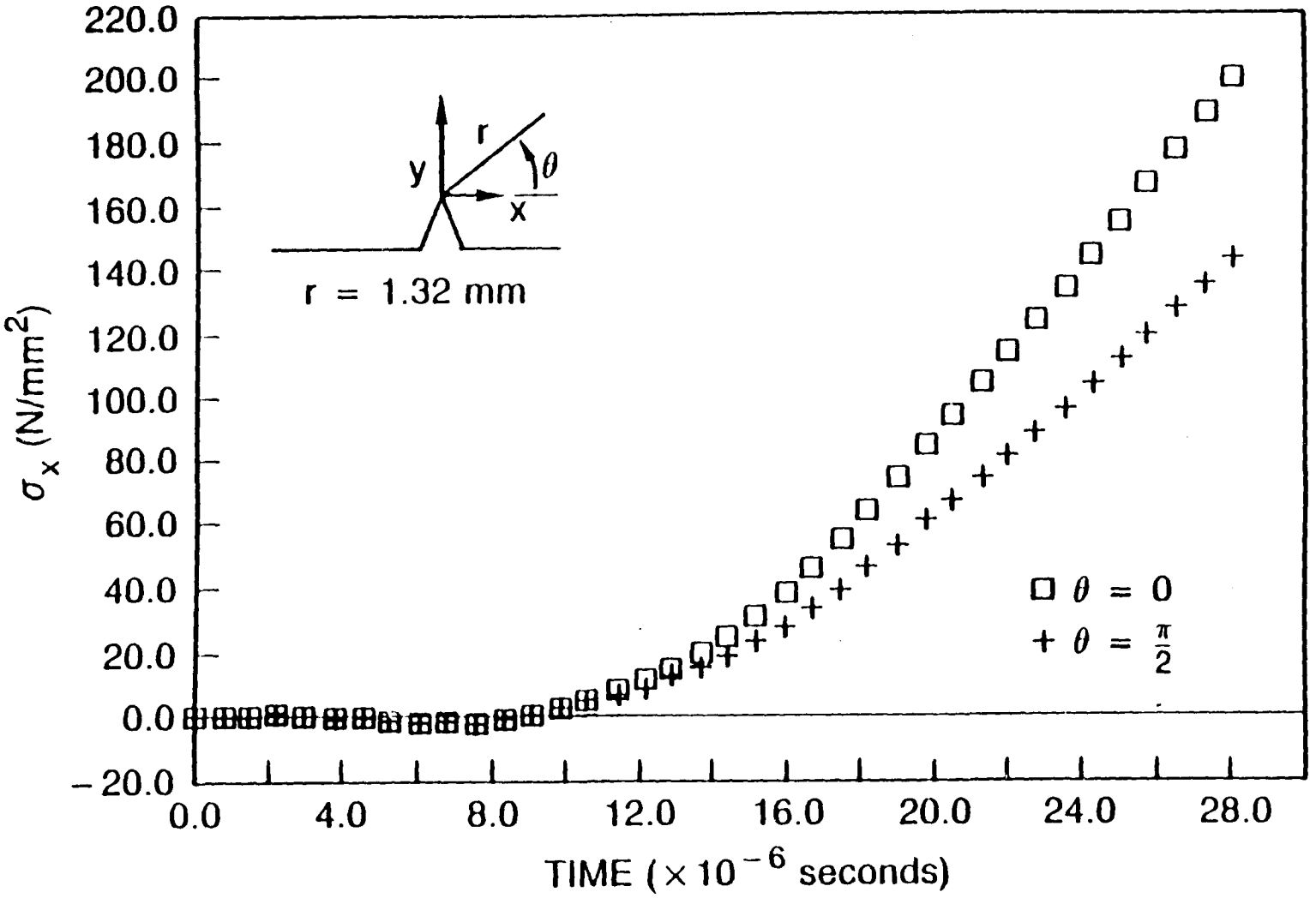

Figure 6 Stress history near notch(crack tip)

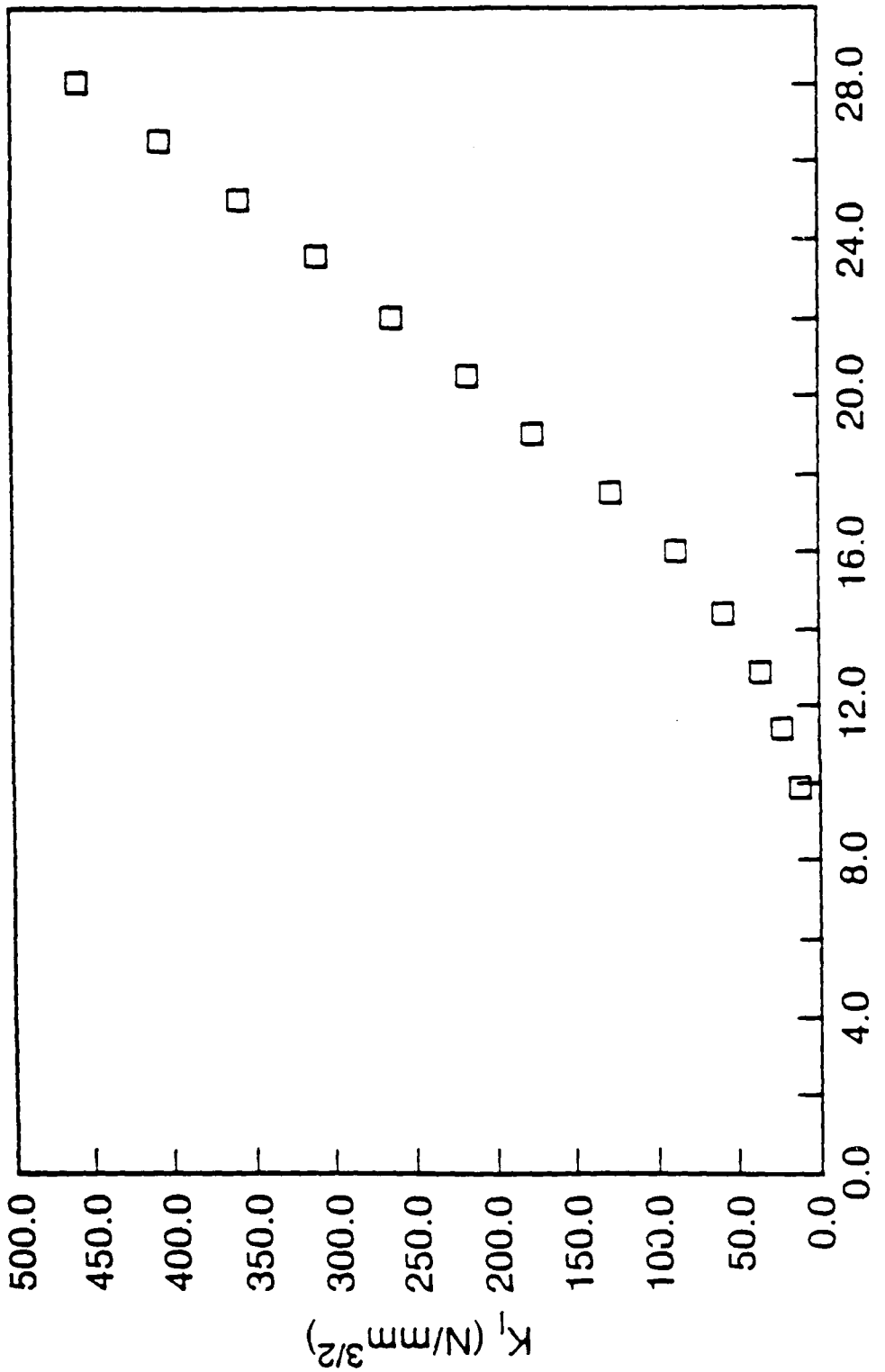

Figure 7 K_I history

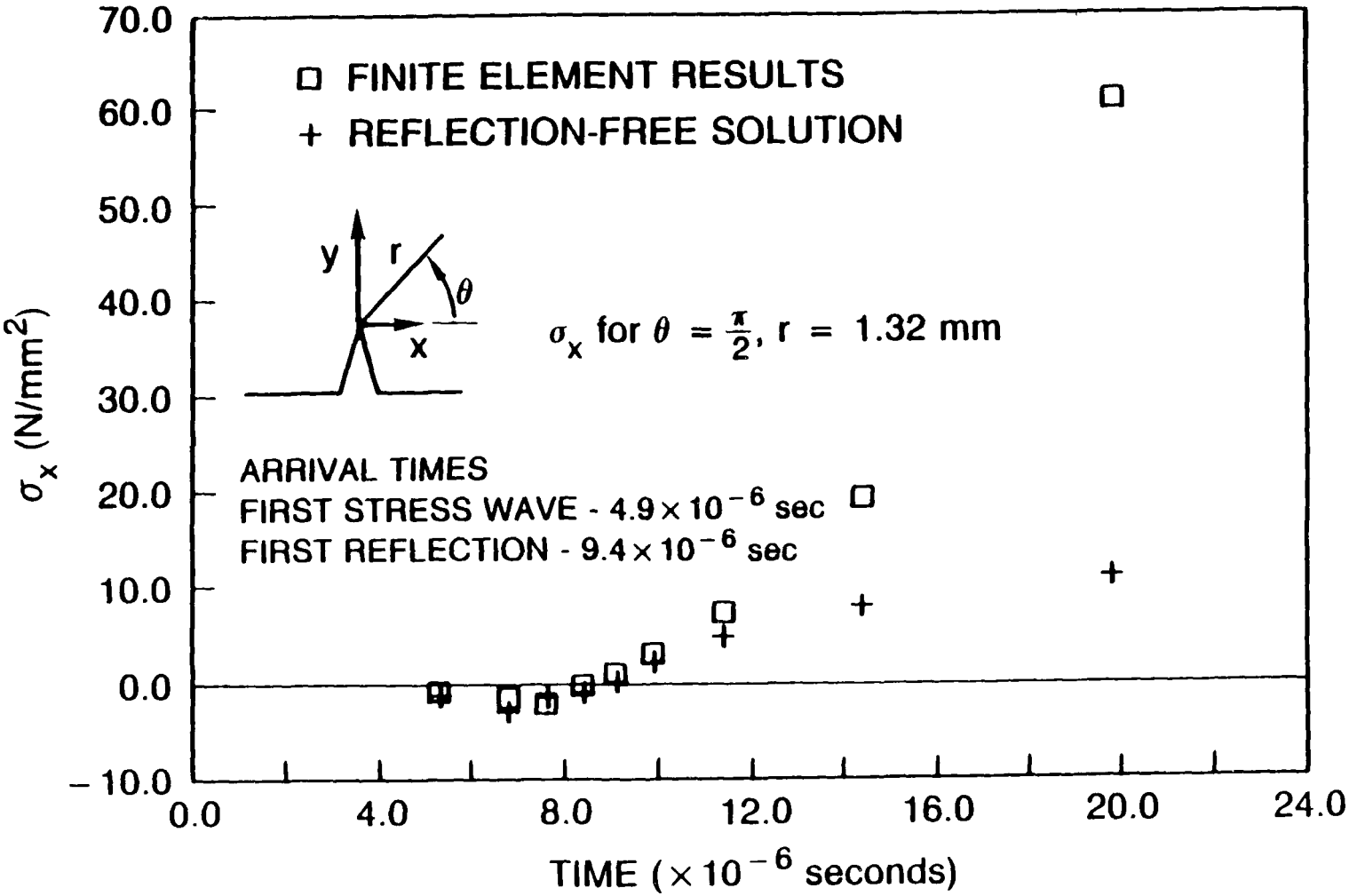

Figure 8 Stress history comparison near notch (crack tip)